

Pressure overloaded right ventricles: a multicenter study on the importance of trabeculae in RV function measured by CMR

Mieke M. P. Driessen · Vivan J. M. Baggen · Hendrik G. Freling ·
Petronella G. Pieper · Arie P. van Dijk · Pieter A. Doevendans · Repke J. Snijder ·
Marco C. Post · Folkert J. Meijboom · Gertjan Tj. Sieswerda · Tim Leiner ·
Tineke P. Willems

Received: 12 September 2013 / Accepted: 12 January 2014 / Published online: 20 January 2014
© Springer Science+Business Media Dordrecht 2014

Abstract Cardiac magnetic resonance (CMR) imaging is the preferred method to measure right ventricular (RV) volumes and ejection fraction (RVEF). This study aimed to determine the impact of excluding trabeculae and papillary muscles on RV volumes and function in patients with RV pressure and/or volume overload and healthy controls and its reproducibility using semi-automatic software. Eighty patients (pulmonary hypertension, transposition of the great arteries after arterial switch operation and after atrial switch procedure and repaired Tetralogy of Fallot) and 20 controls underwent short-axis multislice cine CMR. End diastolic volume (EDV), end systolic volume (ESV), RV mass and RVEF were measured using 2 methods. First, manual contour tracing of RV endo- and epi-cardial

borders was performed. Thereafter, trabeculae were excluded from the RV blood volume using semi-automatic pixel-intensity based software. Both methods were compared using a Student *T* test and 25 datasets were re-analyzed for reproducibility. Exclusion of trabeculae resulted in significantly decreased EDV; ranging from -5.7 ± 1.7 ml/m² in controls to -29.2 ± 6.6 ml/m² in patients after atrial switch procedure. RVEF significantly increased in all groups, ranging from an absolute increase of 3.4 ± 0.8 % in healthy controls to 10.1 ± 2.3 % in patients after atrial switch procedure. Interobserver agreement of method 2 was equal to method 1 for RVEDV, RVESV and RVEF and superior for RV mass. In patients with overloaded RVs exclusion of trabeculae from the blood volume results in a significant change in RV volumes, RVEF and RV mass. Exclusion of trabeculae is

Mieke M. P. Driessen and Vivan J. M. Baggen shared first authorship. Tim Leiner and Tineke P. Willems shared last authorship.

M. M. P. Driessen · F. J. Meijboom · G. Tj. Sieswerda
Department of Cardiology, University Medical Center Utrecht,
University of Utrecht, PO Box 85500, 3508 GA Utrecht,
The Netherlands
e-mail: m.m.p.driessen-2@umcutrecht.nl

F. J. Meijboom
e-mail: f.j.meijboom@umcutrecht.nl

G. Tj. Sieswerda
e-mail: g.t.sieswerda@umcutrecht.nl

M. M. P. Driessen
The Interuniversity Cardiology Institute of The Netherlands
(ICIN), Netherlands Heart Institute, PO Box 19258,
3501 DG Utrecht, The Netherlands

V. J. M. Baggen · P. A. Doevendans · T. Leiner
Department of Radiology, University Medical Center Utrecht,
University of Utrecht, PO Box 85500, 3508 GA Utrecht,
The Netherlands
e-mail: v.j.m.baggen@gmail.com

P. A. Doevendans
e-mail: p.doevendans@umcutrecht.nl

T. Leiner
e-mail: t.leiner@umcutrecht.nl

H. G. Freling · T. P. Willems (✉)
Department of Radiology, University Medical Center
Groningen, University of Groningen, PO Box 30001,
1 Hanzeplein, 9700 RB Groningen, The Netherlands
e-mail: t.p.willems@umcg.nl

H. G. Freling
e-mail: h.g.freling@umcg.nl

P. G. Pieper
Department of Cardiology, University Medical Center
Groningen, University of Groningen, PO Box 30001,
9700 RB Groningen, The Netherlands
e-mail: p.g.pieper@umcg.nl

highly reproducible when semi-automatic pixel-intensity based software is used.

Keywords CMR · Volumetric RV analysis · Congenital heart disease · Pulmonary hypertension · Reproducibility

Introduction

Both in patients with pulmonary hypertension (PH) and in patients with different types of congenital heart disease (CHD), the right ventricle (RV) performs under increased pressure loading. The RV adapts by hypertrophy, however at a certain point the RV is unable to cope with the increased pressures and RV failure will ensue. Consequently, RV function is an important determinant of prognosis and of therapeutic strategy in these patients. For instance, in patients with pulmonary valvular stenosis, timing of intervention is partly dependent on RV function [1]. In patients with PH, deterioration of right ventricular volumes and ejection fraction (RVEF), increased RV end-diastolic volume (RVEDV) and stroke index are associated with poor outcome [2, 3]. Furthermore, for patients with transposition of the great arteries (TGA) after an atrial switch operation, in which the RV supplies the systemic circulation (i.e. systemic RV), decline in RV function is one of the most important clinical problems. Therefore RV volumes and function are frequently used in follow-up of these patients, making accurate and reproducible measurements highly important.

As both 2D and also 3D echocardiography of the RV remain less reproducible than cardiac magnetic resonance imaging (CMR), the latter is still considered to be the reference standard for the quantification of RV volumes and EF [4–7]. Whether trabeculae and papillary muscles should be included or excluded from the blood volume is subject of debate. Throughout literature both methods are used [2, 8–10]. However, many studies have not clearly described whether trabeculae and papillary muscles were

included or excluded from the RV blood volume [11–14]. The impact of trabeculae is assumed to be small in healthy individuals, but Winter et al. showed that exclusion of trabeculae from the RV blood volume resulted in a substantial difference of RVEDV, RVESV and RVEF in patients with a systemic right ventricle [15]. Although theoretically more accurate, Winter et al. also showed that manual tracing of trabeculae has low reproducibility and therefore can be considered less favorable for longitudinal follow-up [5, 15].

Freling et al. [16] recently reported that semi-automatic pixel-intensity based segmentation software is able to exclude trabeculae and papillary muscles from the RV blood volume with high reproducibility in Tetralogy of Fallot (TOF) patients with predominantly volume overloaded RVs. Moreover, this resulted in a substantial difference in RV volumes and RVEF compared to the method which includes these structures in the RV blood volume. In patients with increased RV pressure the trabeculae are likely to be coarser. The impact and reproducibility of excluding trabeculae and papillary muscles with this semi-automatic software in patient groups with RV pressure overload has not been investigated up to now.

The purpose of this multicenter study was to determine the impact of excluding trabeculae and papillary muscles, on RV volumes and function as assessed by CMR in patients with pressure or combined pressure and volume overload of the RV and healthy controls. Secondly, we determine the reproducibility of this methodology when semi-automatic pixel-intensity based software is used.

Methods

Study design and population

One hundred CMR studies were included in the analysis (median age 36.2 years, 51 % male). Four groups of 20 adult patients with pressure overloaded RV's were analyzed: patients with pre-capillary PH, patients with right ventricular outflow tract obstruction (RVOTO) after arterial switch operation (ASO) for TGA, patients with repaired TOF and patients with TGA and atrial switch procedure (Mustard or Senning operation). A reference group of 20 healthy controls was also included.

PH was defined in accordance with the ESC/ESR guidelines as a mean pulmonary artery pressure of ≥ 25 mmHg and a pulmonary capillary wedge pressure of ≤ 15 mmHg [17]. Only patients with pre-capillary (i.e. with arterial vascular changes) PH were included, all were diagnosed with either chronic thrombo-embolic or idiopathic PH. In all patients RV systolic pressure (RVSP) was measured using Doppler echocardiography on the day of

A. P. van Dijk
Department of Cardiology, Radboud University Nijmegen
Medical Center, PO Box 9101, 6500 HB Nijmegen,
The Netherlands
e-mail: A.vanDijk@cardio.umcn.nl

R. J. Snijder
Department of Pulmonology, St. Antonius Hospital,
PO Box 2500, 3430 EM Nieuwegein, The Netherlands
e-mail: r.snijder@antoniuziekenhuis.nl

M. C. Post
Department of Cardiology, St. Antonius Hospital, PO Box 2500,
3430 EM Nieuwegein, The Netherlands
e-mail: m.post@antoniuziekenhuis.nl

Table 1 Basic patient characteristics of each patient group and of healthy controls

	PH n = 20	ASO n = 20	TOF n = 20	Atrial switch n = 20	Controls n = 20
Male gender [n (%)]	7 (35)	11 (55)	11 (55)	12 (60)	10 (50)
Age (years) ^a	55.0 ± 14.1	24.9 ± 4.0	29.1 ± 7.8	33.0 ± 6.3	36.7 ± 10.1
BSA (m ²) ^a	1.93 ± 0.18	1.88 ± 0.18	1.87 ± 0.19	1.96 ± 0.21	1.88 ± 0.21
RVESP (mmHg) ^b	54 (37–65) n = 20	40 (37–53) n = 15	45 (41–50) n = 20	120(106–125) n = 20	–
RVOT (mmHg) ^b	–	35 (29–42) n = 8	33 (30–40) n = 15	–	4 (3–8) n = 20
TR grade [n (%)]					
No/trace	7 (35)	12 (60)	10 (50)	1 (5)	20 (100)
Mild	9 (45)	7 (35)	7 (35)	14 (70)	–
Moderate	4 (20)	1 (5)	3 (15)	4 (20)	–
Severe	–	–	–	1 (5)	–
Missing	–	–	–	–	–
PR grade ^c					
No/trace	14 (70)	14 (70)	9 (45)	13 (65)	20 (100)
Mild	6 (30)	3 (15)	4 (20)	2 (10)	–
Moderate	–	–	–	–	–
Severe	–	–	6 (30)	–	–
Missing	–	2 (10)	1 (5)	5 (25)	–

^a Data presented as mean ± SD

^b Data presented as median (IQR)

^c AR grade in patients after atrial switch

CMR investigation. RVSP was measured using the peak velocity of tricuspid insufficiency plus estimated right atrial pressure. Patients with repaired TOF were included if a RVSP of ≥ 36 mmHg was measured by Doppler echocardiography [18]. Patients after ASO were included if RVSP measured by Doppler echocardiography was ≥ 36 mmHg or if, using Doppler echocardiography, a mild or moderate RVOTO was measured, defined as a maximum gradient of ≥ 25 mmHg. For patients with TGA after atrial switch procedure systolic blood pressure was used to determine RVSP. Basic patient characteristics for each patient group are illustrated in Table 1. Degree of pulmonary (PR) and tricuspid valve regurgitation (TR) were assessed semi-quantitatively with echocardiography, based on color-Doppler and continuous wave Doppler pattern and graded as: none or trace, mild, moderate or severe.

In this retrospective study, MR images from two tertiary referral hospitals were analyzed. One centre contributed 59 patient CMR datasets and 20 control subjects. The second centre provided the remaining 21 patient CMR datasets. The datasets in this study were obtained between May 2008 and July 2012. Prior to analysis, all patient and control data were encoded to preserve anonymity. All CMR datasets were acquired in a routine clinical setting and anonymized

for analysis. The medical ethics committees waived the need for informed consent.

CMR imaging protocol

Datasets were obtained using commercially available 1.5 T MR scanners [Ingenia R4.1.2; Philips Healthcare, Best, The Netherlands (n = 79); Magnetom Sonata, Siemens Healthcare; (n = 7) and Magnetom Avanto; Siemens Healthcare, Erlangen, Germany (n = 14)]. For all studies dedicated chest or torso phased array parallel-imaging capable surface coils were used with 12–28 elements. CMR images were acquired during repeated end-expiratory breath holds. Cine images were acquired using a retrospectively gated balanced steady state free precession sequence with 25–30 cardiac phases per cardiac cycle. Slice thickness used were 6 with 4 mm gap (n = 21) or 8 with 0 mm gap (n = 79). Sequences included multi-slice, multi-phase cine short-axis, longitudinal four-chamber, vertical two-chamber and RV outflow views. The multi-slice cine short-axis acquisitions were planned from above the mitral valve up to and including the cardiac apex. The following ranges of other scan parameters were used: TR 2.7–3.4 ms; TE 1.1–1.7 ms; flip angle 80°–90°; matrix 171–192; voxel

size: $1.25 \times 1.25 \times 8.0$ mm and $1.7 \times 1.7 \times 6.0$ mm. Parallel imaging factors varied between 0–3.

CMR image analysis

Image analysis was performed using Qmass MR Research edition version 7.4.14.0 (Medis, Leiden, the Netherlands) [16]. Segmentation was performed on end-diastolic and end-systolic phases only.

The end-diastolic and end-systolic phase was selected by visual assessment as the phase with the largest and smallest RV cavity sizes respectively, taking into account the longitudinal 4-chamber, vertical 2-chamber and RV outflow tract as reference views. If visual assessment was difficult, multiple frames were contoured to determine the correct end-diastolic or end-systolic phase. Using a previously described RV analysis protocol the RV epicardial and endocardial contours were manually traced from the most apical to the most basal short-axis slice [19]. Only the

portion of the outflow tract below the pulmonary valve was included in the blood volume in the basal slice in which the pulmonary valve was visible. If more than 50 % of the tricuspid annulus or atrium was visible in a basal slice the valve area was excluded from the blood volume. Epicardial and endocardial contours overlapped at valve borders and septum, as the septum was considered part of the left ventricle. For patients with systemic RV, the septum was considered part of the RV and included in the RV myocardial volume.

Based on the methodology described above, two methods were used for determining RV volumes, function and mass. With method 1 trabeculae and papillary muscles were included in the blood volume. With method 2, trabeculae and papillary muscles were excluded from the blood volume (Fig. 1) and added to the myocardial volume. For both methods the volume between the endo- and epi-cardial contour was considered myocardial volume. Selection of trabeculae and papillary muscles was done

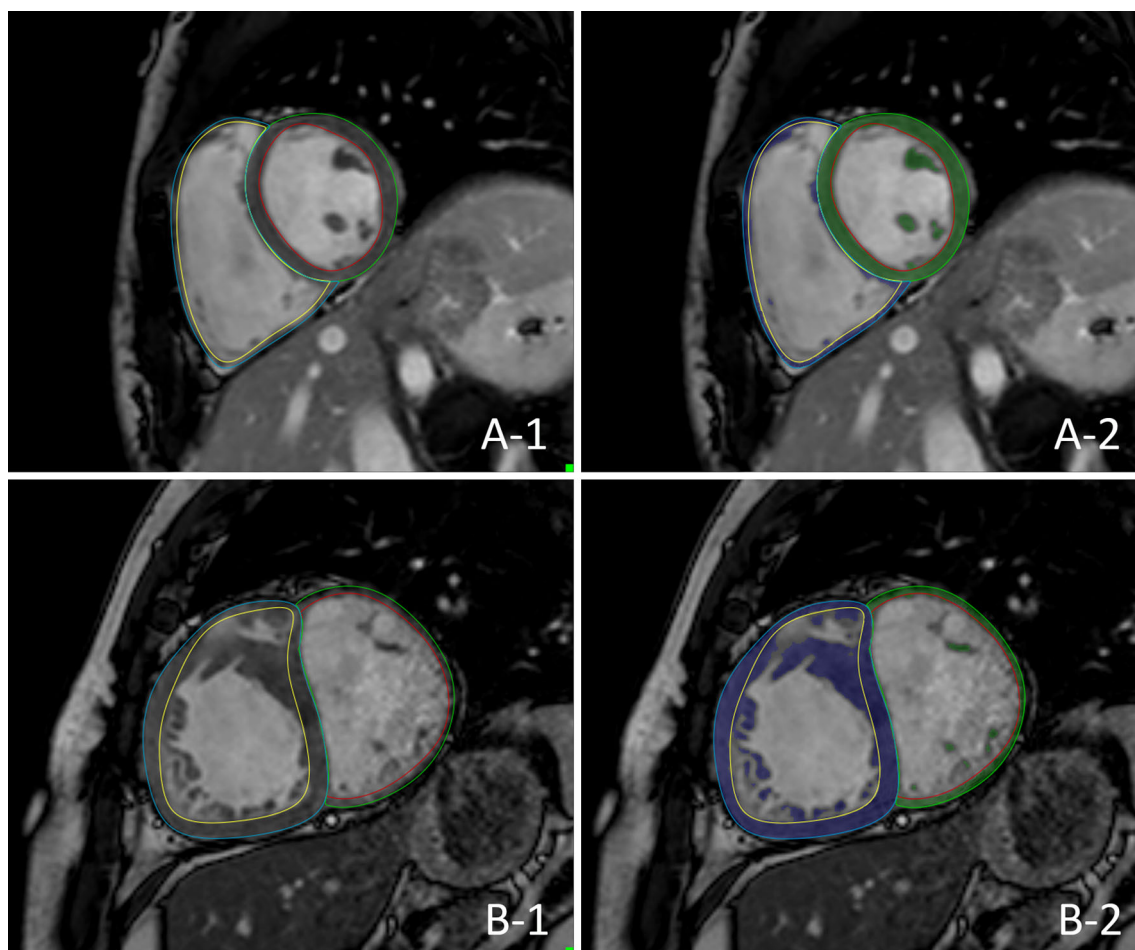


Fig. 1 RV contour tracing only (A-1 and B-1) and with semi-automatic selection of trabeculae (A-2 and B-2). Two methods of measuring RV volumes in a healthy control (a) and patient after atrial

switch procedure (b). Method 1: inclusion trabeculae in the blood volume (a-1 and b-1); Method 2: exclusion of trabeculae from the blood volume, using identical endocardial contours (a-2 and b-2)

using semi-automatic pixel-intensity based segmentation software. The segmentation software is based on the signal intensity distribution of MR images and has been described in detail by Freling et al. [16]. In brief, voxels within the epicardial contour are classified as either blood volume or myocardial volume according to their signal intensity, taking into account spatial variations in signal intensity. Based on this algorithm, trabeculae and papillary muscles were excluded from the blood volume and included in the myocardial volume. The algorithm works similar for images generated by the different scanners used in this study. It was a possibility to manually change the threshold for every slice, in order to select the same trabeculae in end-diastole and end-systole. Observers selected only trabeculae with signal intensity similar to the intensity of RV myocardium. Individual voxels could also be selected or deselected in case of artifacts due to nonlaminar flow.

For both methods, RV volumetric parameters were calculated by the sums of the traced contours multiplied by slice thickness in all short-axis slices. For method 1 the volume of trabeculae and papillary muscles was included in the RV blood volume and for method 2 this was excluded from the blood volume. Stroke volume (SV) was defined as the difference between end diastolic volume and end systolic volume. All volumetric data were indexed for body surface area (BSA), which was calculated using the Dubois–Dubois formula ($0.20247 \times \text{height (m)}^{0.725} \times \text{weight (kg)}^{0.425}$). EF was calculated by $\text{SV/EDV} \times 100 \%$. For method 1 myocardial volume was defined as epicardial minus the endocardial contour, for method 2 end-diastolic trabecular volume was added to the myocardial volume. RV mass was quantified by multiplying the specific density of myocardium (1.05 g/ml) with the end-diastolic myocardial volume.

Reproducibility

Intraobserver reproducibility of both methods was assessed by re-analyzing five randomly selected CMR datasets from every patient group, as well as the healthy control subjects by the primary observer. In total 25 datasets were reanalyzed. To determine interobserver variability a second observer re-analyzed the same 25 datasets. Observers were unaware of the results of the first analysis and there was an interval of at least two weeks between the first and second analysis. The observers had equal experience in RV volumetric analysis and received the same training for Qmass MR research edition.

Statistical analysis

Continuous data were expressed as median and interquartile range (IQR) or mean value \pm standard deviation

(SD) as appropriate. Mean differences \pm SD between method 1 and 2 was calculated for RVEDV/m^2 , RVESV/m^2 , RVSV/m^2 , RVEF and RV mass/m^2 , using paired Student's *T* test. Differences in RVEDV/m^2 , RVESV/m^2 and RVEF found in the patient groups were compared to the healthy control group using a one-way ANOVA with posthoc Dunnett's test. For the one-way ANOVA data underwent logarithmic transformation if necessary (i.e. if homogeneity of variances was unequal). Intra- and inter-observer agreement were assessed using Bland–Altman plots and intraclass correlation coefficients (ICC). Paired Student's *T* test was used to test for significant differences between observer 1 and 2 and between the first and second measurements of observer 1. Mean differences \pm SD were calculated for all measurements. Lastly to compare reproducibility of both methods the inter- and intra-observer agreement coefficient of method 1 and 2 were calculated for each measurement. The $AC_{\text{intra/inter}}$ was calculated using the following formula: $AC_{\text{intra/inter}} = 100 \times (1 - 2 \times |Obs1 - Obs2| / (Obs1 + Obs2))$; in which Obs1 and 2 are the first and the second observation (or observer). The $AC_{\text{intra/inter}}$ calculated for method 1 and 2 were compared using a paired Wilcoxon signed rank test. Using this formula the relative observer differences of both methods are compared. Using a Bonferonni correction for multiple measurements *p* values of <0.01 were considered statistically significant. All data analysis was performed in IBM SPSS statistics version 20.0 (IBM SPSS, Chicago, IL, USA).

Results

Exclusion of trabecular volume

RVEDV/m^2 , RVESV/m^2 , RV EF and RV mass/m^2 measured including (method 1) and excluding (method 2) RV trabeculae from the RV blood volume are listed in Table 2. For all patient groups and for healthy controls, exclusion of trabeculae and papillary muscles from the blood volume resulted in significantly decreased RVEDV/m^2 and RVESV/m^2 and a significantly increased RVEF and RV mass/m^2 (Table 2). Of note, the differences in EDV/m^2 , ESV/m^2 , RVEF , and RV mass between both methods were most pronounced in the patients after atrial switch procedure and least pronounced in the PH patients, with mean absolute differences in EF of 10.1 ± 2.3 and $4.7 \pm 1.6 \%$, respectively. In healthy controls an absolute increase in RVEF of $3.4 \pm 0.8 \%$ was measured. Of note, the differences in EDV/m^2 , EDV/m^2 , RVEF and RV mass were significantly larger in all patients groups compared to the healthy controls ($p < 0.01$).

Table 2 RV volumes and function

	PH (mean ± SD)	ASO (mean ± SD)	TOF (mean ± SD)	Atrial switch (mean ± SD)	Controls (mean ± SD)
RVEDV (ml/m²)					
Method 1	117.4 ± 31.8	99.4 ± 23.3	147.0 ± 42.5	139.9 ± 33.6	96.9 ± 18.9
Method 2	105.1 ± 28.4	88.3 ± 21.2	124.8 ± 38.0	110.7 ± 28.7	91.2 ± 17.8
Difference	-12.3 ± 4.6*	-11.1 ± 3.3*	-22.2 ± 6.0*	-29.2 ± 6.6*	-5.7 ± 1.7*
RVESV (ml/m²)					
Method 1	75.4 ± 30.0	50.1 ± 13.3	85.5 ± 27.8	85.9 ± 26.2	47.5 ± 11.5
Method 2	62.7 ± 25.9	39.2 ± 11.3	63.7 ± 23.2	57.1 ± 21.7	41.6 ± 10.5
Difference	-12.7 ± 4.8*	-10.9 ± 3.3*	-21.8 ± 6.0*	-28.8 ± 6.5*	-5.9 ± 1.5*
SV (ml/m²)					
Method 1	42.0 ± 7.9	49.3 ± 11.7	61.5 ± 19.4	54.0 ± 14.9	49.4 ± 8.6
Method 2	42.4 ± 8.0	49.2 ± 11.5	61.0 ± 19.6	53.6 ± 14.7	49.6 ± 8.6
Difference	-0.4 ± 0.6**	-0.2 ± 0.6	-0.4 ± 0.8**	-0.4 ± 0.9	0.2 ± 0.5
RV mass (g/m²)					
Method 1	18.5 ± 5.5	20.1 ± 5.0	25.4 ± 7.1	43.3 ± 9.1	13.0 ± 3.0
Method 2	31.4 ± 9.8	31.1 ± 7.5	48.7 ± 12.3	73.9 ± 15.4	19.0 ± 4.2
Difference	12.9 ± 4.9*	11.0 ± 4.8*	23.3 ± 6.3*	30.6 ± 6.9*	6.0 ± 1.8*
RVEF (%)					
Method 1	37.2 ± 8.5	49.6 ± 5.0	42.1 ± 6.9	39.2 ± 7.8	51.3 ± 3.8
Method 2	41.9 ± 9.1	55.8 ± 5.1	49.4 ± 12.3	49.3 ± 9.7	54.7 ± 4.1
Difference	4.7 ± 1.6*	6.1 ± 1.7*	7.2 ± 1.7*	10.1 ± 2.3*	3.4 ± 0.8*

RV volumes, mass and ejection fraction measured with inclusion (method 1) and exclusion of trabeculae from the RV blood volume (method 2). All volumetric data are indexed for BSA

* $p < 0.001$ using paired Student's T test; ** $p < 0.05$ using paired Student's T test

Table 3 Inter- and intra-observer agreement

	Interobserver (obs 2–obs 1 ^I)			Intraobserver (obs 1 ^{II} –obs 1 ^I)		
	ICC	Mean difference ± SD	p value	ICC	Mean difference ± SD	p value
RVEDV (ml/m²)						
Method 1	0.981	-2.4 ± 6.7	0.089	0.990	2.8 ± 5.1	0.012
Method 2	0.987	1.8 ± 4.5	0.059	0.985	3.0 ± 5.0	0.006
RVESV (ml/m²)						
Method 1	0.970	-2.3 ± 5.2	0.039	0.982	1.1 ± 4.2	0.209
Method 2	0.974	1.7 ± 3.5	0.027	0.969	1.0 ± 3.8	0.194
RVEF (%)						
Method 1	0.934	0.9 ± 2.6	0.086	0.965	0.4 ± 1.8	0.241
Method 2	0.934	-0.5 ± 2.6	0.354	0.954	0.6 ± 2.2	0.189
RVmass (g/m²)						
Method 1	0.965	5.8 ± 3.5	0.000	0.983	0.5 ± 2.3	0.283
Method 2	0.993	1.4 ± 2.6	0.012	0.990	0.3 ± 3.2	0.694

Intra-class correlation coefficient and the absolute mean difference ± SD for all measurements

Obs2 second observer, Obs1^I first measurement of primary observer, Obs1^{II} second measurement of primary observer

p value obtained using paired student T test

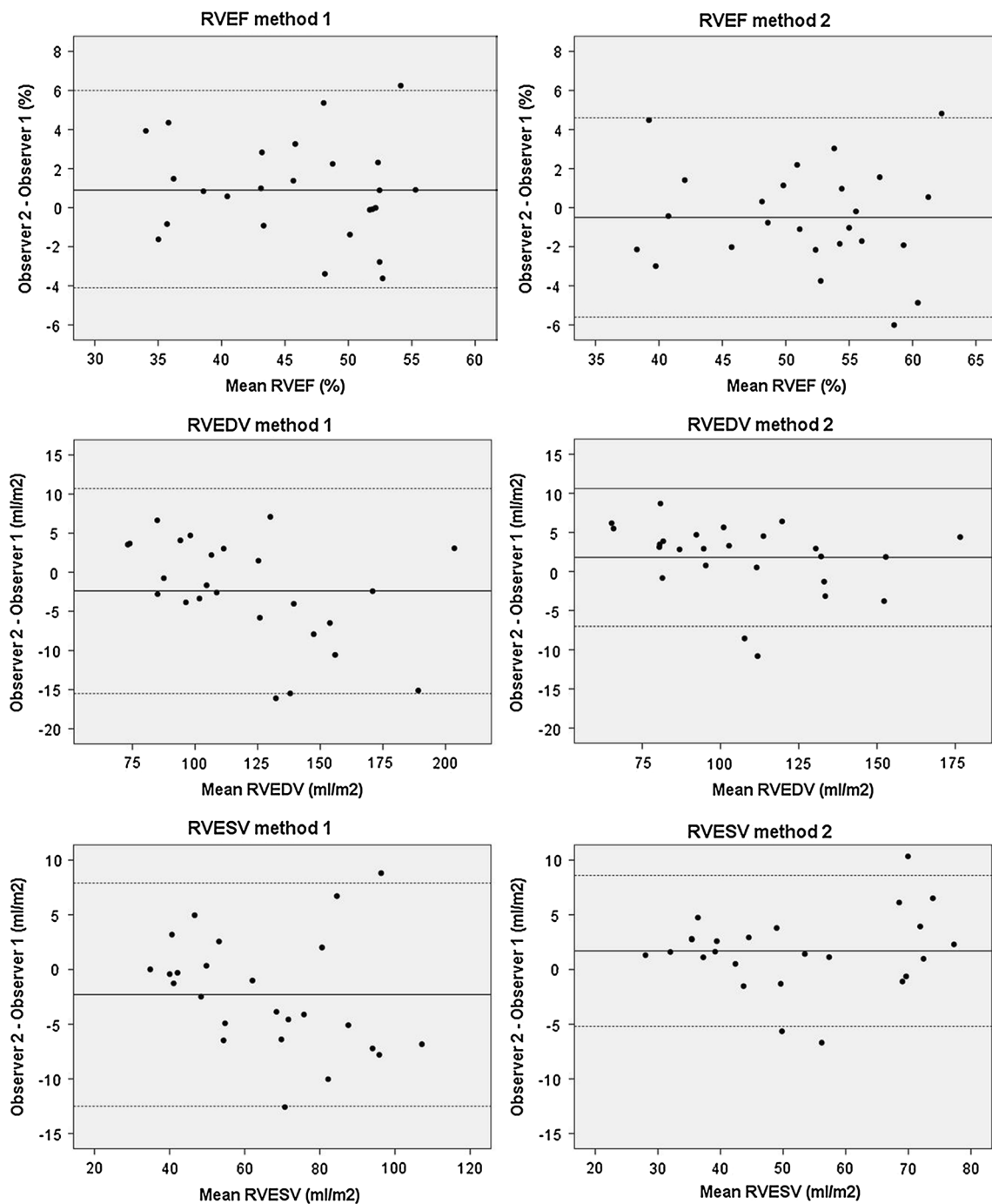


Fig. 2 Bland–Altman plots for method 1 and method 2. Bland–Altman plots showing the mean value of both observers on the x-axis and absolute differences between the observers on the y-axis for each paired observation. Limits of agreement are defined as ± 2 SD

Reproducibility

For both methods inter- and intra-observer agreement was high in all measurements, as illustrated by high ICCs with small limits of agreement (Table 3; Fig. 2). For both methods, RVEDV, RVESV and RV mass showed significant differences between repeated measurements.

However, mean differences were small and considered not clinically relevant. In Fig. 2, Bland–Altman plots show interobserver variability for RVESV, RVEDV and RVEF for both methods. For RVEDV, RVESV and RV mass the limits of agreement were narrower when trabeculae and papillary muscles were excluded from the RV blood volume (method 2). The *AC_{intra/inter}* of all measurements

was not statistically significantly different for RVEDV, RVESV and RVEF ($p > 0.1$). Method 2 had a significantly better AC_{inter} than method 1 for RV mass measurement, with a median (IQR) AC_{inter} of respectively 94.1 (92.1–97.1) % and 77.2 (72.1–82.6) %.

Discussion

Exclusion of trabeculae and papillary muscles resulted in substantial alterations of RV volumes, RVEF and RV mass in a wide range of patient populations with pressure and volume overloaded RVs. Furthermore, we found that these differences in RV parameters vary widely depending on the exact condition underlying RV overload. Although prior studies already established this fact in general terms, the major impediment to widespread adoption of this method in clinical practice was the lack of a fast and reproducible way to measure the exact amount of RV trabeculae and papillary muscles. We found that exclusion of RV trabeculae using semi-automatic pixel-intensity based software resulted in fast and highly reproducible RV measurements. This is opposed to manual tracing of trabeculae which has previously been shown to be unreliable [15, 20].

Accurate and reproducible measurement of RV volume and function is mandatory because of the prognostic and therapeutic implications in patients with PAH and CHD [1, 3, 21, 22]. The current study underscores that exclusion of trabeculae has a significant impact on RV volumes, RVEF and RV mass in both CHD and PAH patients with overloaded RVs. Moreover, the impact of excluding trabeculae varied widely between patient groups, from a change in RVEDV of -12.3 ± 4.6 ml/m² in PH patients to -29.2 ± 6.6 ml/m² in patients with a systemic RV. Healthy controls also exhibited significant differences in all RV measurements, but these were significantly smaller ($p < 0.01$) compared to the differences observed in patient groups. Consequently, RV volume and function in most patients will be closer to or in the normal range after exclusion of trabeculae from the RV blood volume.

Currently, there is no clear standard for RV volumetric analysis or consensus on how trabecular structures should be handled. Major obstacles to exclude trabeculae and papillary muscles from the RV blood volume have been the time investment of performing manual tracing of these structures and the low reproducibility [15, 20]. Several studies in CHD patients differ on the point of including or excluding RV trabeculae and papillary muscles from the RV blood volume [3, 4, 11, 12, 20, 22, 23] or are not clear about the methodology used [13, 14]. In the current study we found that using semi-automatic pixel-intensity based segmentation software results in highly reproducible RV volumetric measurements. Because inclusion or exclusion

of trabeculae has a major impact on RV parameters as measured with CMR, studies using different methodologies are incomparable. Application of the method described in this study may be a step forward to achieve uniformity of RV volumetric measurements, which is important to compare the effect of interventions aimed at preserving or improving RV function. However, there are only few reports using this new methodology and it is of great importance that new studies are undertaken to determine clinically relevant cut-off values using this semi-automated method.

When comparing the current study to prior studies investigating the impact of trabeculae and papillary muscles on RV volume and function, some important differences can be observed. Winter et al. studied 29 patients with systemic right ventricles and found an increase in RVEF of 7.4 ± 3.9 % compared to 10.1 ± 2.3 % in our report. In contrast to our results, which are based on semi-automated pixel-intensity based segmentation, manual exclusion of trabeculae was substantially less reproducible in the study of Winter et al. [15]. Moreover, both our study and the study by Freling et al. [16] even demonstrated a higher reproducibility for respectively RV mass and both RVEDV and RV mass using this semi-automatic method to exclude trabeculae compared to only endocardial contour tracing. We attribute this finding to observer variation in handling of trabeculae adjacent to the endocardial border. This can result in small differences for endocardial contour tracing, which will be rectified if all trabeculae are excluded. Sievers et al. [24] studied the effect of trabeculae on RV volumes in healthy controls and reported a difference in RVEF of only 1.72 % compared to 3.4 ± 0.8 % in our study, however baseline RVEDV values also differed considerably with ours, indicating that these study populations are not comparable. Freling et al. [16] investigated a different group of TOF patients, with volume overloaded RV's using the same software package as described in the current study and found a similar increase in RVEF of 7 ± 4 versus 7 ± 2 % in our study.

The current study only focused on one of the possible sources of error in RV volumetric assessment with CMR. An important source of error remains basal slice selection and delineation of the tricuspid valve. In this study a short-axis orientation for RV volumetric measurement was used as this is standard practice in our hospitals. Axial orientation, however, might result in higher reproducibility than short-axis orientation in CHD patients with severely dilated RVs, decreasing the difficulty of valve delineation in the basal slices [25, 26]. To minimize errors at the tricuspid and pulmonic valve, images were cross linked to RV 2-chamber, 4-chamber and RV outflow tract views. Furthermore only a small portion of the patients had severely dilated RVs, therefore it is unlikely that the slice

orientation would have resulted in important differences for the current study. The impact and reproducibility of the semi-automatic software used in the current study will likely be similar in axial slice orientation, as the software is not restricted by geometric assumptions and uses signal intensity to select trabeculae. Finally, another source of error might be inadequate selection of the RV end-systolic frame. In daily practice both RV ESV and LV ESV are often assessed in the LV end-systolic frame. However in patients with CHD, who often have right bundle branch block, timing of the RV end-systolic frame can be delayed compared to the LV end-systolic frame [27]. Therefore RV end-diastolic and end-systolic phase was based solely on RV cavity size.

Study limitations

This study is unable to determine whether including or excluding trabeculae best represents true RV volumes, as a gold standard in vivo is lacking. Because the SV remains equal with both methodologies other CMR measurements are unable to serve as a reference standard. However, theoretically exclusion of trabeculae is more accurate as these do not contribute to RV blood volumes in end-diastole or end-systole.

Furthermore no invasive measurements were available to determine the true RV pressure in these patients. Therefore estimations of RVESP and RVOT gradient based on Doppler-derived flow velocities were used, which might not always be accurate and have limitations. Nonetheless these are the best available non-invasive alternatives to assess degree of RV pressure overload or RVOT stenosis.

Conclusion

Exclusion of trabeculae and papillary muscles has a significant impact on measured RV volumes, mass and EF. The magnitude of the differences varies between patient groups and is significantly larger in all investigated patient groups with overloaded RVs than in healthy controls. Importantly, exclusion of trabeculae with semi-automatic pixel-intensity based software is highly reproducible and superior compared to manual contour tracing for RV mass.

Conflict of interest None.

References

- Baumgartner H, Bonhoeffer P, De Groot NM, de Haan F, Deanfield JE, Galie N, Gatzoulis MA, Gohlke-Baerwolf C, Kaemmerer H, Kilner P, Meijboom F, Mulder BJ, Oechslin E, Oliver JM, Serraf A, Szatmari A, Thaulow E, Vouhe PR, Walma E, Task Force on the Management of Grown-up Congenital Heart Disease of the European Society of Cardiology (ESC), Association for European Paediatric Cardiology (AEPC), ESC Committee for Practice Guidelines (CPG) (2010) ESC Guidelines for the management of grown-up congenital heart disease (new version 2010). *Eur Heart J* 31:2915–2957
- van de Veerdonk MC, Kind T, Marcus JT, Mauritz GJ, Heymans MW, Bogaard HJ, Boonstra A, Marques KM, Westerhof N, Vonk-Noordegraaf A (2011) Progressive right ventricular dysfunction in patients with pulmonary arterial hypertension responding to therapy. *J Am Coll Cardiol* 58:2511–2519
- van Wolferen SA, Marcus JT, Boonstra A, Marques KM, Bronzwaer JG, Spreeuwenberg MD, Postmus PE, Vonk-Noordegraaf A (2007) Prognostic value of right ventricular mass, volume, and function in idiopathic pulmonary arterial hypertension. *Eur Heart J* 28:1250–1257
- Valsangiacomo Buechel ER, Mertens LL (2012) Imaging the right heart: the use of integrated multimodality imaging. *Eur Heart J* 33:949–960
- Kilner PJ, Geva T, Kaemmerer H, Trindade PT, Schwitter J, Webb GD (2010) Recommendations for cardiovascular magnetic resonance in adults with congenital heart disease from the respective working groups of the European Society of Cardiology. *Eur Heart J* 31:794–805
- van der Zwaan HB, Geleijnse ML, McGhie JS, Boersma E, Helbing WA, Meijboom FJ, Roos-Hesselink JW (2011) Right ventricular quantification in clinical practice: two-dimensional vs. three-dimensional echocardiography compared with cardiac magnetic resonance imaging. *Eur J Echocardiogr* 12:656–664
- Iriart X, Montaudon M, Lafitte S, Chabaneix J, Reant P, Balbach T, Houle H, Laurent F, Thambo JB (2009) Right ventricle three-dimensional echocardiography in corrected tetralogy of fallot: accuracy and variability. *Eur J Echocardiogr* 10:784–792
- Beerbaum P, Barth P, Kropf S, Sarikouch S, Kelter-Kloeping A, Franke D, Gutberlet M, Kuehne T (2009) Cardiac function by MRI in congenital heart disease: impact of consensus training on interinstitutional variance. *J Magn Reson Imaging* 30:956–966
- Rominger MB, Bachmann GF, Pabst W, Rau WS (1999) Right ventricular volumes and ejection fraction with fast cine MR imaging in breath-hold technique: applicability, normal values from 52 volunteers, and evaluation of 325 adult cardiac patients. *J Magn Reson Imaging* 10:908–918
- Lorenz CH, Walker ES, Morgan VL, Klein SS, Graham TP Jr (1999) Normal human right and left ventricular mass, systolic function, and gender differences by cine magnetic resonance imaging. *J Cardiovasc Magn Reson* 1:7–21
- Oosterhof T, van Straten A, Vliegen HW, Meijboom FJ, van Dijk AP, Spijkerboer AM, Bouma BJ, Zwinderman AH, Hazekamp MG, de Roos A, Mulder BJ (2007) Preoperative thresholds for pulmonary valve replacement in patients with corrected tetralogy of Fallot using cardiovascular magnetic resonance. *Circulation* 116:545–551
- Therrien J, Provost Y, Merchant N, Williams W, Colman J, Webb G (2005) Optimal timing for pulmonary valve replacement in adults after tetralogy of Fallot repair. *Am J Cardiol* 95:779–782
- Lidegran M, Odhner L, Jacobsson LA, Greitz D, Lundell B (2000) Magnetic resonance imaging and echocardiography in assessment of ventricular function in atrially corrected transposition of the great arteries. *Scand Cardiovasc J* 34:384–389
- Lee C, Kim YM, Lee CH, Kwak JG, Park CS, Song JY, Shim WS, Choi EY, Lee SY, Baek JS (2012) Outcomes of pulmonary valve replacement in 170 patients with chronic pulmonary regurgitation after relief of right ventricular outflow tract obstruction: implications for optimal timing of pulmonary valve replacement. *J Am Coll Cardiol* 60:1005–1014

15. Winter MM, Bernink FJ, Groenink M, Bouma BJ, van Dijk AP, Helbing WA, Tijssen JG, Mulder BJ (2008) Evaluating the systemic right ventricle by CMR: the importance of consistent and reproducible delineation of the cavity. *J Cardiovasc Magn Reson* 10:40
16. Freling HG, van Wijk K, Jaspers K, Pieper PG, Vermeulen KM, van Swieten JM, Willems TP (2013) Impact of right ventricular endocardial trabeculae on volumes and function assessed by CMR in patients with tetralogy of Fallot. *Int J Cardiovasc Imaging* 29:625–631
17. Task Force for Diagnosis and Treatment of Pulmonary Hypertension of European Society of Cardiology (ESC), European Respiratory Society (ERS), International Society of Heart and Lung Transplantation (ISHLT), Galie N, Hoeper MM, Humbert M, Torbicki A, Vachiery JL, Barbera JA, Beghetti M, Corris P, Gaine S, Gibbs JS, Gomez-Sanchez MA, Jondeau G, Klepetko W, Opitz C, Peacock A, Rubin L, Zellweger M, Simonneau G (2009) Guidelines for the diagnosis and treatment of pulmonary hypertension. *Eur Respir J* 34:1219–1263
18. Rudski LG, Lai WW, Afilalo J, Hua L, Handschumacher MD, Chandrasekaran K, Solomon SD, Louie EK, Schiller NB (2010) Guidelines for the echocardiographic assessment of the right heart in adults: a report from the American Society of Echocardiography endorsed by the European Association of Echocardiography, a registered branch of the European Society of Cardiology, and the Canadian Society of Echocardiography. *J Am Soc Echocardiogr* 23:685–713
19. Prakken NH, Velthuis BK, Vonken EJ, Mali WP, Cramer MJ (2008) Cardiac MRI: standardized right and left ventricular quantification by briefly coaching inexperienced personnel. *Open Magn Reson J* 1:104–111
20. Papavassiliu T, Kuhl HP, Schroder M, Suselbeck T, Bondarenko O, Bohm CK, Beek A, Hofman MM, van Rossum AC (2005) Effect of endocardial trabeculae on left ventricular measurements and measurement reproducibility at cardiovascular MR imaging. *Radiology* 236:57–64
21. Warnes CA (2009) Adult congenital heart disease importance of the right ventricle. *J Am Coll Cardiol* 54:1903–1910
22. Knauth AL, Gauvreau K, Powell AJ, Landzberg MJ, Walsh EP, Lock JE, del Nido PJ, Geva T (2008) Ventricular size and function assessed by cardiac MRI predict major adverse clinical outcomes late after tetralogy of Fallot repair. *Heart* 94:211–216
23. Helbing WA, Rebergen SA, Maliepaard C, Hansen B, Ottenkamp J, Reiber JH, de Roos A (1995) Quantification of right ventricular function with magnetic resonance imaging in children with normal hearts and with congenital heart disease. *Am Heart J* 130:828–837
24. Sievers B, Kirchberg S, Bakan A, Franken U, Trappe HJ (2004) Impact of papillary muscles in ventricular volume and ejection fraction assessment by cardiovascular magnetic resonance. *J Cardiovasc Magn Reson* 6:9–16
25. Clarke CJ, Gurka MJ, Norton PT, Kramer CM, Hoyer AW (2012) Assessment of the accuracy and reproducibility of RV volume measurements by CMR in congenital heart disease. *JACC Cardiovasc Imaging* 5:28–37
26. Fratz S, Schuhbaeck A, Buchner C, Busch R, Meierhofer C, Martinoff S, Hess J, Stern H (2009) Comparison of accuracy of axial slices versus short-axis slices for measuring ventricular volumes by cardiac magnetic resonance in patients with corrected tetralogy of fallot. *Am J Cardiol* 103:1764–1769
27. Freling HG, Pieper PG, Vermeulen KM, van Swieten JM, Sijens PE, van Veldhuisen DJ, Willems TP (2013) Improved cardiac MRI volume measurements in patients with tetralogy of Fallot by independent end-systolic and end-diastolic phase selection. *PLoS ONE* 8:e554–e562